European Journal of Pharmacology 632 (2010) 93–102

Contents lists available at ScienceDirect

European Journal of Pharmacology

journal homepage: www.elsevier.com/locate/ejphar

Immunopharmacology and Inflammation

KR-003048, a potent, orally active inhibitor of p38 mitogen-activated protein kinase

Antonio Garrido Montalban, Erik Boman, Chau-Dung Chang, Susana Conde Ceide, Russell Dahl, David Dalesandro, Nancy G.J. Delaet, Eric Erb, Justin Ernst, Andrew Gibbs, Jeffrey Kahl, Linda Kessler, Jan Lundström, Stephen Miller, Hiroshi Nakanishi, Edward Roberts, Eddine Saiah, Robert Sullivan, Zhijun Wang, Christopher J. Larson *

Drug Discovery, Kemia, Inc., San Diego, CA, United States

ARTICLE INFO

Article history:
Received 11 April 2009
Received in revised form 9 December 2009
Accepted 20 January 2010
Available online 2 February 2010

Keywords:
p38
Kinase
Inhibitor
TNF (Tumor necrosis factor)
Arthritis

ABSTRACT

The tumor necrosis factor-α (TNF-α) cytokine, secreted by activated monocytes/macrophages and T lymphocytes, is implicated in several diseases, including rheumatoid arthritis, chronic obstructive pulmonary disease, inflammatory bowel disease, and osteoporosis. Monocyte/macrophage production of TNF-α is largely driven by p38α mitogen-activated protein kinase (MAP kinase), an intracellular soluble serine–threonine kinase. p38α MAP kinase is activated by growth factors, cellular stresses, and cytokines such as TNF-α and interleukin-l (IL-I). The primary contribution of p38α activation to excess TNF-α in settings of both chronic and acute inflammation has instigated efforts to find inhibitors of this enzyme as possible therapies for associated disease states. Analogue design, synthesis, and structure–activity studies led to the identification of 5-tert-butyl-N-cyclopropyl-2-methoxy-3-{2-[4-(2-morpholin-4-yl-ethoxy)-naphthalen-1-yl]-2-oxo-acetylamino}-benzamide (KR-003048) as a potent inhibitor of the p38 MAP kinase signaling pathway *in vitro* and *in vivo*. The inhibition *in vitro* of human p38α enzyme activity and lipopolysaccharide (LPS)-induced p38 activation and subsequent TNF-α release is described. KR-00348 was demonstrated to be a potent inhibitor of inflammatory cytokine production *ex vivo* in rat and human whole blood, and showed good oral bioavailability. Additionally, efficacy in mouse and rat models of acute and chronic inflammation was obtained. KR-003048 possessed therapeutic activity in acute models, demonstrating substantial inhibition of carrageenan-induced paw edema and *in vivo* LPS-induced TNF release at 30 mg/kg p.o. Collagen-induced arthritis in mice was significantly inhibited by 10 and 30 mg/kg doses of KR-003048. Evidence for disease-modifying activity in this model was indicated by histological evaluation of joints.

1. Introduction

Rheumatoid arthritis is a progressively worsening autoimmune disease of unknown origin in which the immune system attacks joint tissue, causing joint damage and inflammation. Many studies have shown that tumor necrosis factor-α (TNFα) is a principal mediator of inflammation in rheumatoid arthritis, contributing to joint effusion, synovial proliferation, and bone and cartilage damage in addition to systemic inflammation (Bingham, 2002). The proinflammatory cytokine interleukin 1 (IL-1) is also a significant factor in the pathology of rheumatoid arthritis, contributing primarily to joint destruction. Mediators released during inflammatory disease states initiate intracellular signaling cascades regulated by kinases and phosphatases (Herlaar and Brown, 1999). The mitogen-activated protein kinases (MAP kinases) are key components of such signaling cascades at which various extracellular stimuli converge to initiate inflammatory cellular responses. Several subgroups can be discriminated within the MAP kinase family, including the p42/44 extracellular signal-related kinases, c-Jun N-terminal kinase, and p38 MAP kinase (Han et al., 1994; Kyriakis et al., 1994; Lee et al., 1994; Kyriakis and Avruch, 1996). Each pathway has multiple isoforms, each of which may play different roles and be differentially expressed in various tissues. The p38 MAP kinase has been identified as an important regulator of the coordinated release of cytokines (Fig. 1) by immunocompetent cells and the functional response of neutrophils to inflammatory stimuli (Herlaar and Brown, 1999; Ono and Han, 2000). Four isozymes of p38 have been cloned and characterized, including the ubiquitously expressed p38α and p38β. p38γ is primarily expressed in skeletal muscle, and p38δ is highly distributed within lung, kidney, endocrine glandular, and small intestinal tissues. In inflammatory cells, p38α is the most prominent.

Many different stimuli can activate p38 MAP kinase. These include lipopolysaccharide (LPS) and other bacterial products, cytokines such as TNF-α and IL-1β, growth factors, and stresses such as heat shock, hypoxia, and ischemia/reperfusion ((Herlaar and Brown, 1999); (Ono and Han, 2000)). One of the cellular responses after p38 MAP kinase

* Corresponding author. Exelixis, Inc., 4757 Nexus Centre Drive, San Diego, CA 92121, United States. Tel.: +1 858 458 4504; fax: +1 858 458 4501.
E-mail address: clarson@exelixis.com (C.J. Larson).

0014-2999/$ – see front matter © 2010 Elsevier B.V. All rights reserved.
doi:10.1016/j.ejphar.2010.01.011

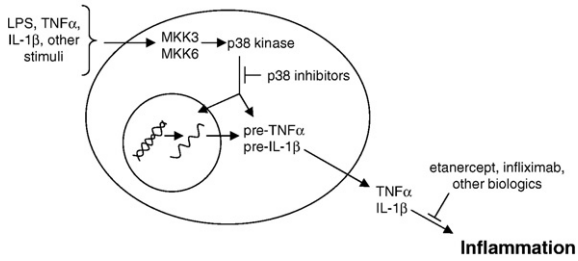

Fig. 1. Mediators released during inflammatory disease states initiate intracellular signaling cascades regulated by kinases and phosphatases. The mitogen-activated protein kinases (MAP kinases) are key components of such signaling cascades at which various extracellular stimuli converge to initiate inflammatory cellular responses. Several subgroups can be discriminated within the MAP kinase family, including the p42/44 extracellular signal-related kinases, c-Jun N-terminal kinase, and p38 MAP kinases. Each pathway has multiple isoforms, each of which may play different roles and be differentially expressed in various tissues.

activation is release of proinflammatory cytokines such as TNFα, IL-l, interleukin-6 (IL-6), and interleukin-8 (IL-8). In addition, p38 MAP kinase positively regulates a variety of genes involved in inflammation, such as TNFα, IL-1, IL-6, IL-8, cyclooxygenase-2 (COX-2), and collagenase-1 (COX-1) and -6 (COX-6) (Ono and Han, 2000). The p38 pathway mediates multiple cellular functions in addition to the propagation of inflammation, including migration (Hannigan et al., 2001; Kotlyarov et al., 2002), survival (Kontoyiannis et al., 2002), and cell death (Wang et al., 2002). To accomplish its many functions, p38 phosphorylates several transcription factors, including myocyte enhancer factor 2A (MEF2A), myocyte enhancer factor 2C (MEF2C), ETS-domain protein (Elk4/SAP1), C/EBP-homologous protein (CHOP), signal transducer and activator of transcription 1 (STAT1), nuclear factor of activated T cells (NFAT), caudal type homeo box transcription factor 2 (CDX3), and activating transcription factor 2 (ATF-2), and it activates several downstream kinases via phosphorylation, including mitogen- and stress-activated kinases 1 and 2 (MSK1/2), MAP kinase signal-integrating kinase (MNKl), mitogen-activated protein kinase kinase 2 (MK2), mitogen-activated protein kinase kinase 3 (MK3), and mitogen-activated protein kinase kinase 5 (MK5) (Shi and Gaestel, 2002). p38α has been shown to contain a binding groove capable of recognizing docking sites present on both upstream kinase activators and downstream substrates, including MEF2A, MEF2C, mitogen-activated protein kinase 3b (MKK3b), mitogen-activated protein kinase 6 (MKK6), and the MK's.

While MAP kinase inhibition as a therapeutic approach has many potential problems–kinases are the principal regulatory mechanisms for intracellular signaling and are so numerous they comprise 2% of the genome–dual inhibitors of p38-α/β have shown efficacy in arthritic and inflammatory diseases in clinical trials. Patients with active Crohn's disease and rheumatoid arthritis exhibit increased activation of p38 MAP kinase (Redlich et al., 2003; Waetzig et al., 2002; Pargellis and Regan, 2003), thus validating this as a potential novel target for the treatment of inflammatory disorders (Saklatvala, 2004). It has been demonstrated that small molecule inhibitors of p38 significantly reduce the release of both of these cytokines from human monocytes, a highly valuable feature with the synergistic effects of anti-IL-1β and anti-TNF-α therapy becoming increasingly clear. Numerous commercial drug discovery teams have advanced p38 inhibitors into development, and small molecule p38 inhibitors VX-745, VX-702, and BIRB796 have reported results. VX-745 demonstrated efficacy on clinical endpoints in a Phase II rheumatoid arthritis trial (Weisman et al., 2002), and VX-702 reported significant inhibition of C-reactive protein (CRP) induction during percutaneous intervention (PCI) procedures (de Winter et al., 2005). Positive outcomes from a Phase II rheumatoid arthritis trial with VX-702 have been reported, but to date have only appeared in a company press release (www.vpharm.com). Disappointingly, another p38 inhibitor BIRB796 appeared to lack efficacy against clinical measures of Crohn's disease (Schreiber et al., 2006), resulting in a mixed overall picture of the potential for modulation of this target to address the medical needs of patients with autoimmune conditions.

Kemia has developed and implemented a general strategy for identifying potent, selective compounds for optimization into drug candidates. Applied to p38, this approach led to the rapid identification of several series of drug leads for p38α, which are selective against other enzymes tested, including other p38 isoforms. We report here the results of optimization–*via* identification, structure–activity relationship development, synthesis, and enzymatic and cellular profiling–of one such series of p38α inhibitors. Another member of this series is currently undergoing Phase II clinical trials for multiple indications.

2. Materials and methods

2.1. Materials

Lipopolysaccharide (*Salmonella typhimurium*) was purchased from Sigma (St. Louis, MO, USA), SB203580 (4-(4-Fluorophenyl)-2-(4-methylsulfinyl phenyl)-5-(4-pyridyl) 1H-imidazole) hydrochloride from Calbiochem (San Diego, CA, USA). BIRB796 was synthesized internally. hTNFα Duoset ELISA kit was purchase from R&D Systems (Minneapolis, MN).

2.2. In vitro kinase assays

p38α MAP kinase assay was performed by MDS Pharma. Briefly, p38α (human recombinant from *E. coli*) was pre-incubated for 15 min at 25 °C with or without test compound or vehicle (dimethyl sulfoxide (DMSO), 1% final concentration), and then 10 μg/ml myelin basic protein (MBP) was incubated for 60 min at 25 °C (50 mM HEPES, pH 7.4, 20 mM $MgCl_2$, 0.2 mM Na_3VO_4, 1 mM DTT). The amount of phosphorylated MBP substrate was determined by enzyme-linked immunosorbent assay (ELISA) quantitation.

2.3. TNF cellular secretion assay

7×10^4 THP-1 cells (human monocyte cell line from ATCC) in low serum growth medium (1% fetal calf serum) were pre-treated with the appropriate concentration of compound in 0.1% dimethyl sulfoxide (DMSO) for 1 h prior to addition of 1 μg/ml lipopolysaccharide (Sigma). 18–20 h after LPS treatment the cells were pelleted and the media was assayed for human TNFα levels using the R&D Systems hTNFα Duoset ELISA kit.

2.4. p38 phosphorylation assay

10^5 THP-1 cells were plated at 10^5/well in a 96well plate and grown in 20 nM phorbol 12-myristate 13-acetate (PMA) for 48 h in order to induce differentiation. Media was replaced with low serum (1% fetal calf serum) medium for 4 h prior to compound addition. Cells were pre-treated with the appropriate concentration of compound for 30 min., then 1 μg/ml LPS was added for 30 min. Cells were lysed and assayed for phospho-p38 activity using the Phospho-p38 ELISA kit from R&D Systems.

2.5. Inhibition of TNF secretion by whole blood

Before extracting blood media was prepared by warming to 37 °C. Blood was drawn no more than 60 min. before using in assay. Blood was prepared in a 3:2 ratio blood to 1% fetal calf serum/media. Warm media was used to prepare a 6× dilution of LPS. The final concentration in the assay was 1 μg/μl. Samples were vortexed or mixed with 10 ml disposable pipette, then incubated at 37 °C and 5%

CO2 for 4 h on a plate shaker. A CisBio Human TNFα homogeneous time resolved fluorescence (HTRF) detection kit was used for this assay. Detection was carried out in an LJL 384 well Black H.E. microplate. After 4 hours of incubation, the blood assay plate was removed from the 37 °C incubator and spun in a plate centrifuge at 2500 rpm for 10 min. 7.5 µl of each well of supernatant was transferred to a well on the 384 well plate. Plates were incubating for at least 3 h in the dark before reading. Read on LJL Analyst.

2.6. Pharmacokinetics in rodents

2.6.1. KR-003048 and BIRB796 in rats

After preparation, dosing solutions were kept refrigerated at 4 °C and protected from light whenever possible. Following administration procedures, remaining solutions were stored frozen at approximately −20 °C. Concentration and stability of the test compound dosing solutions were assayed before administration. Concentration was determined by a liquid chromatography-mass spectrometry (LC-MS) method. Stability was assayed by high-pressure liquid chromatography-ultraviolet detection (HPLC-UV) methods. Male Lewis rats were used, at 250 g at dosing. Groups of four animals received single i.v. or p.o. doses of the test compound. The animals were assigned to the different dose groups in order to balance, as far as possible, the distribution of body weights. Dose volumes administered were calculated based on the body weight recorded just prior to administration. The animals were not in the fasting state, although food was removed approximately 2 h prior to administration. Intravenous doses were given in a tail vein, and blood samples were collected *via* saphenous vein. Serial samples were collected from each animal pre-dose and then at 0.10, 0.25, 0.5, 1.0, 2.0, 4.0, and 7 h. Blood samples were processed for serum and the serum fractions stored at −20 °C until assays were performed.

2.7. Inhibition of TNF release in rodents

Male Lewis rats (about 250 g at dosing) were pre-treated with vehicle or test compound 30 min before (p.o.) a LPS challenge dose. One hour after the challenge dose, animals were bled and sacrificed. Dose volumes administered were calculated based on the average body weight recorded just prior to administration. The animals were not in the fasting state, although food was removed approximately 3 h prior to administration of pretreatment doses. The LPS challenge dose was given by intraperitoneal injection at a dose of 1.0 mg/kg. Blood samples were collected by cardiac puncture and processed for serum. The serum fractions were stored at 4 °C if being processed same day, or −20 °C until assays were performed. Prior to blood collection the animals were anesthetized *via* inhaled isoflurane then euthanized. The concentration of test articles in serum was determined at Kémia Inc. by a LC-MS method. Plasma levels of TNFα were determined at Kémia by ELISA methods.

2.8. Inhibition of acute paw swelling in rats

Lambda carrageenan was dissolved to 10 mg/ml in deionized water and stored at 4 °C. Sprague–Dawley rats (Harlan Sprague Dawley, female, 170–190 g, R# 1442, P.O. no. 163327, Texas) were received, individually examined, and housed in cages of 5 rats each. Each animal was in apparent good health: no signs of clinical stress. Indomethacin (10 mg, Sigma I-109, Lot 48H7975) was dissolved in 2 ml of 100 mM sodium bicarbonate in a sonicating water bath. Thirty-six rats were selected at random from the animals available and housed in groups of eight animals/cage. The rats were ear-notched for identification purposes and the right hind foot was marked below the ankle joint to ensure consistency of paw volume measurements. Initial rat paw volumes were measured and the groups of animals were injected intraperitoneally or intravenously. Animals were observed after vehicle/agent administration for adverse effects. Fifteen minutes after the vehicle/agent administration, the animals were anesthetized and carrageenan (0.1 ml of a 10 mg/ml solution) was injected in the subplantar region of the right hind paw. At 2, 4 and 6 h post carrageenan injection the paw volumes were re-measured in the water plethysmograph. After the 6 h time point, all animals were anesthetized (SOP 1810) and exsanguinated. The blood was collected in heparinized Vacutainer tubes, separated by centrifugation and the plasma transferred to labeled 15 ml conical tubes. Serum was prepared. The serum was stored at −20 °C. The samples were kept at 4 °C as much as possible until they were frozen.

2.9. Inhibition of collagen-induced arthritis in mice

Mice were received and placed in quarantine for at least three days. On Day 0, mice were weighed and separated into treatment groups: non-diseased controls that received no adjuvant (10 mice), and diseased mice (20 mice/treatment group). Mice were anesthetized, shaved at the base of tail, and injected (id) with adjuvant (50 µl/mouse; 100 µg/mouse collagen; 100 µg/mouse M. tuberculosis H37Ra) using 1 ml syringe fitted with a 26 gauge (G) needle. On Day 21, adjuvant was prepared by emulsifying (homogenizer) a 1:1 combination of collagen and M. tuberculosis H37Ra. Adjuvant was injected id (50 µl/mouse; 100 µg/mouse collagen; 100 µg/mouse M. tuberculosis H37Ra) using a 1 ml syringe fitted with a 26 G needle. On Days 22–27, mice were scored daily for macroscopic signs of arthritis. Each paw received a score: 0 = no visible effects of arthritis: 1 = edema and/or erythema of one digit; 2 = edema and/or erythema of two joints; 3 = edema and/or erythema of more than two joints; 4 = severe arthritis of the entire paw and digits. Arthritic index was calculated by adding all individual paw scores (maximum arthritic index = 16), and then recorded. On Day 28, mice were sorted into treatment groups (10 mice/group) based upon arthritic index. Each treatment group had a similar average arthritic index, and a similar range of arthritic indices. Dosing by the oral route was initiated on this day and continued for 14 days. On Days 29–42, mice were dosed, and any adverse effects of test agent administration were recorded. Macroscopic signs of arthritis were also scored daily, with each paw receiving a score. On Day 43, after the final scoring of macroscopic signs of arthritis, mice were exsanguinated, and blood collected in heparinized tubes. Livers were removed, and their weights recorded. Limbs were removed and immersed in four volumes of 10% buffered formalin. Limbs were subsequently decalcified, blocked, sectioned, hematoxylin and eosin (H&E) stained, and read by a pathologist.

3. Results

3.1. Modeling

Because of their widespread potential applications in numerous clinical indications, inhibitors of p38 kinases have been discovered and developed by numerous commercial and academic entities (Diller et al., 2005; Dominguez et al., 2005; Hynes and Leftheri, 2005; Michelotti et al., 2005; Natarajan and Doherty, 2005; Pargellis and Regan, 2003). The chemical architectures underlying these various efforts can be roughly divided into six broad categories (Fig. 2A): (i) pyridinyl imidazoles and derivatives with heterocyclic replacements of the imidazole core, as exemplified by the pioneering Smith Kline series and the more recent RWJ-67657; (ii) pyrimidopyridazinones and related bicyclic 6,6-heterocyclic structures, as exemplified by compounds from Vertex (VX-745) and Merck; (iii) N, N′-diaryl ureas, as exemplified by BIRB796 from Boehringer Ingelheim; (iv) aromatic carboxamides such as those recently publicized by Astra-Zeneca and Bristol-Myers Squibb; (v) indole amides, such as those described by J&J/Scios; and (vi) diaryl ketones, exemplified by the structures claimed by LEO Pharma. As described elsewhere (Garrido Montalban

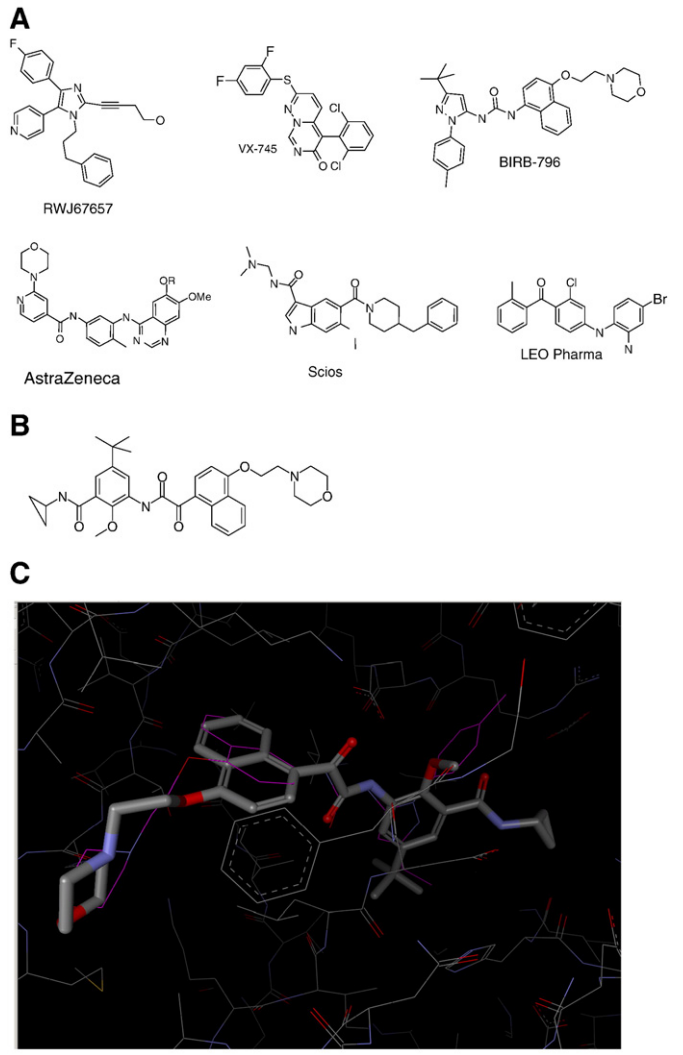

Fig. 2. A. p38 inhibitors. The chemical architectures of most p38 inhibitors can be divided into six broad categories: (i) pyridinyl imidazoles and derivatives with heterocyclic replacements of the imidazole core, as exemplified by the pioneering Smith Kline series and the more recent RWJ-67657; (ii) pyrimidopyridazinones and related bicyclic 6,6-heterocyclic structures, as exemplified by compounds from Vertex (VX-745) and Merck; (iii) N, N′-diaryl ureas, as exemplified by BIRB796 from Boehringer Ingelheim; (iv) aromatic carboxamides such as those recently publicized by Astra-Zeneca and Bristol-Myers Squibb; (v) indole amides, such as those described by J&J/Scios; and (vi) diaryl ketones, exemplified by the structures claimed by LEO Pharma. B. KR-003048. Analogue design, synthesis, and structure–activity studies led to the identification of 5-tert-butyl-N-cyclopropyl-2-methoxy-3-{2-[4-(2-morpholin-4-yl-ethoxy)-naphthalen-1-yl]-2-oxo-acetylamino}-benzamide (KR-003048) as a potent inhibitor of the p38 MAP kinase signaling pathway *in vitro* and *in vivo*. C. KR-003048 Bound to p38α. KR-003048 is oriented orthogonally to ATP and there is no structural overlap between the atoms of KR-003048 and ATP in the model. The protein conformation to which KR-003048 could be best fitted was one in which a conformational change for residues in the conserved Asp-Phe-Gly (DFG) motif in the active site has been assumed.

et al., 2008), medicinal chemistry efforts at Kemia have yielded a chemical scaffold distinct from these four classes, yet closest in relative terms to the diaryl ureas such as BIRB796. Indeed, molecular modeling of the Kemia compound described herein, KR-003048 (Fig. 2B), predicts a mode of binding to p38α strikingly similar to that observed in the X-ray crystal structure of BIRB796 cocrystallized with p38α. In both cases, the compounds utilize an allosteric binding pocket on the kinase that is spatially distinct from the adenosine triphosphate (ATP) pocket (Fig. 2C). In the model, KR-003048 overlaps well with the predicted binding of BIRB796 to p38; the latter's binding mode has been confirmed by X-ray crystallography (Regan et. al., 2003). The protein conformation to which KR-003048 could be best fitted was one in which a conformational change for residues in the conserved Asp-Phe-Gly (DFG) motif in the active site has been assumed.

In protein Ser/Thr kinase structures solved to date, the DFG motif populates a conformation with the Phe residue buried in a hydrophobic pocket in the groove between the two lobes of the kinase (DFG-in conformation). The amino acids in this pocket are very conserved among the kinases. In the model of the complex with KR-003048, however, the Phe side chain shifts to a new location (DFG-out conformation). In this new location, one face of the Phe side chain packs close to KR-003048 while the other face is exposed to solvent. This shift of the Phe side chain allows a large hydrophobic pocket in the kinase to form, and the t-butyl group of KR-003048 inserts into this pocket. Structure–activity relationship (SAR) studies demonstrated that exchanging the t-butyl group for smaller moieties produced several log reductions in activity, providing strong support for the importance of hydrophobic interactions in the binding pocket assumed in this model (Garrido Montalban et al., 2008). Workers at Boehringer Ingelheim have convincingly argued that p38 inhibitors such as KR-003048 and BIRB796 function as noncompetitive enzyme inhibitors by stabilizing a conformation of the protein (DFG-out) incompatible with ATP binding (Pargellis, et al., 2002).

3.2. Inhibition of cytokine release and p38 kinase activity

As a rapid, robust, quantitative measure of inhibition of stimulated cytokine release in a relevant cellular context, the human monocytic cell line THP-1 was exposed to LPS in the presence or absence of p38 MAP kinase inhibitors KR-003048, SB203580, and BIRB796 (Fig. 3). As would be expected from literature reports (Pargellis and Regan, 2003; Regan et al., 2002, 2003), BIRB796 was the most potent compound in this cellular context, with an IC_{50} of 12 nM under these conditions. SB203580 and KR-003048 displayed an apparent potency in this assay that was roughly one half-log higher, with IC_{50}s of 45 and 49 nM, respectively.

To confirm that KR-003048 was inhibiting p38 kinase activity, the compound was pre-incubated with purified p38 kinase before incubating with substrate MBP and measuring the extent of phosphorylation (Fig. 4). The IC_{50} value for KR-003048 under our conditions was 22 nM. This compared favorably with the measured

A

Inhibition of LPS-induced TNF secretion (nM)

SB203580			BIRB796			KR-003048		
mean	S.D.	n	mean	S.D.	n	mean	S.D.	n
45	11	3	12	6	32	49	36	11

B

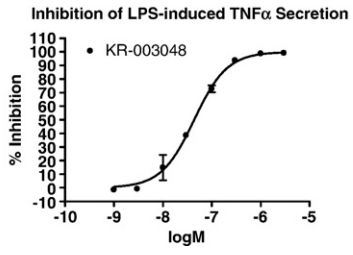

Fig. 3. A. Inhibition of LPS-induced TNFα secretion human monocytic cell line THP-1 was exposed to LPS in the presence or absence of p38 MAP kinase inhibitors KR-003048, SB203580, and BIRB796, and IC_{50}s calculated. Tabulated data for all experiments performed with each compound are shown. B. Inhibition of LPS-induced TNFα secretion human monocytic cell line THP-1 was exposed to LPS in the presence or absence of p38 MAP kinase inhibitors KR-003048, SB203580, and BIRB796, and IC_{50}s calculated. A representative curve for KR-003048 inhibition of LPS-induced TNFα secretion is shown.

A

Inhibition of p38a (nM)

SB203580			BIRB796			KR-003048		
mean	S.D.	n	mean	S.D.	n	mean	S.D.	n
33	14	5	35	21	56	22	12	6

B

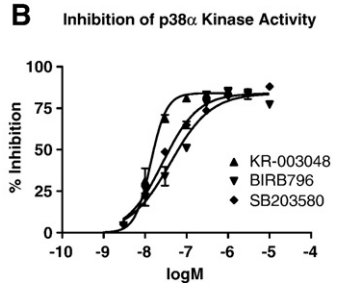

Fig. 4. A. Inhibition of p38α kinase activity. Compound was pre-incubated with purified p38 kinase before incubating with substrate MBP, measuring the extent of phosphorylation, calculating the percentage inhibition of kinase activity based on the minimum and maximum phosphorylation signals detected without and with kinase in the absence of inhibitor, and calculating IC_{50}s. Tabulated data for all experiments performed with each compound are shown. B. Inhibition of p38α kinase activity. Compound was pre-incubated with purified p38 kinase before incubating with substrate MBP, measuring the extent of phosphorylation, calculating the percentage inhibition of kinase activity based on the minimum and maximum phosphorylation signals detected without and with kinase in the absence of inhibitor, and calculating IC_{50}s. Representative curves for inhibition of p38α kinase activity by each compound from individual experimental runs are shown.

A

Inhibition of LPS-induced phosphorylation of p38a (nM)

SB203580			BIRB796			KR-003048		
mean	S.D.	n	mean	S.D.	n	mean	S.D.	n
2500	3700	5	17	3	3	47	13	2

B

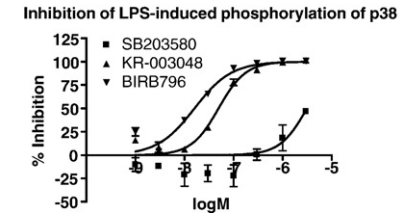

Fig. 5. A. Inhibition of LPS-induced phosphorylation of p38α. Cells were pre-treated with the appropriate concentration of compound for 30 min., then 1 μg/ml LPS was added for 30 min. Cells were lysed and assayed for phospho-p38 activity using the Phospho-p38 ELISA kit from R&D Systems. Tabulated data for all experiments performed with each compound are shown. B. Inhibition of LPS-induced phosphorylation of p38α. Cells were pre-treated with the appropriate concentration of compound for 30 min., then 1 μg/ml LPS was added for 30 min. Cells were lysed and assayed for phospho-p38 activity using the Phospho-p38 ELISA kit from R&D Systems. Representative curves for inhibition of LPS-induced phosphorylation of p38α by each compound from individual experimental runs are shown.

IC_{50} of 35 nM for BIRB796. The literature standard SB203580 yielded a potency of 33 nM under these conditions.

3.3. Inhibition of phosphorylation of p38

MKK3 and MKK6 are two closely related dual specificity protein kinases that activate p38 MAP kinase. Both enzymes phosphorylate and activate p38 MAP kinase at its activation site Thr-Gly-Tyr but do not phosphorylate or activate the other two MAP kinases, extracellular signal-regulated kinases 1 and 2 (ERK1/2) or c-Jun N-terminal kinase (JNK). Phosphorylation of p38 MAP kinase greatly stimulates its ability to phosphorylate protein substrates such as ATF-2, MBP, and Ets like gene 1 (Elk-1) by stabilizing the catalytically active conformation of p38 relatively to the catalytically much less active, DFG-out conformation. As noted above, workers at Boehringer Ingelheim have shown via X-ray crystallography that BIRB796 functions as a noncompetitive enzyme inhibitor by stabilizing an allosteric conformation of the protein (DFG-out) that is incompatible with ATP binding. In contrast, the prototypical Smith Kline p38 inhibitor SB203580 binds to the catalytically active, DFG-in conformation of p38 (Tong, et al., 1997). This is consistent with its mechanism as a competitive inhibitor that binds in space overlapping with that which would otherwise be occupied by ATP. Fig. 5 shows that BIRB796, by stabilizing p38 in the DFG-out conformation, can also prevent phosphorylation of p38 by its upstream activating kinases with a potency of 21 nM IC_{50}, nearly identical to those for inhibition of p38's catalytic activity as measured as 12 nM in cells (Fig. 3) and 35 nM biochemically (Fig. 4). This is consistent with its mechanism as a noncompetitive inhibitor, as measurements of the ability of p38 to be phosphorylated and measurements of p38's catalytic activity both merely read out the underlying conformational state of the protein. In contrast, the competitive inhibitor SB203580 binds to the same conformational state of p38 as does ATP–the catalytically active, phosphorylatible conformation–and thus does not inhibit phosphorylation of p38 by upstream kinases with any significant potency. KR-003048 displays an IC_{50} of 50 nM inhibiting the phosphorylation of p38, very similar to its IC_{50} for inhibition of p38's catalytic activity as measured both in cells (Fig. 3) and biochemically (Fig. 4), 49 and 22 nM, respectively.

3.4. Inhibition of cytokine release from rat and human whole blood

Inhibition of cytokine release can also be measured from samples of whole blood. Analogous to experiments with immortalized cells, human or rodent whole blood diluted with media was exposed to LPS in the presence or absence of p38 MAP kinase inhibitors KR-003048, SB203580, and BIRB796. KR-003048 and BIRB796 were similarly potent in their inhibition of TNF release from both rat and human blood (Fig. 6). Thus, KR-003048 showed an IC_{50} of 1222 nM for TNF inhibition from human blood and 2571 nM from rat blood, while BIRB796 showed an IC_{50} of 579nM for TNF inhibition from human blood and 974 nM from rat blood. Both compounds were more potent in inhibiting TNF release from human than rat blood, though observed experimental differences were small and likely not significant. Interestingly, while SB203580 displayed an IC_{50} of 225 nM for inhibition of TNF from human blood, its inhibition of TNF from rat blood showed an IC_{50} of 1691 nM, almost one log less in potency and a more significant difference than that observed with the other two compounds.

KR-003048, SB203580, and BIRB796 all were more potent in their inhibition of IL-1β secretion by LPS-stimulated blood than in the corresponding inhibition of TNF secretion. Thus, KR-003048 showed an IC_{50} of 408 nM for IL-1β inhibition in human blood and 2067 nM for IL-1β inhibition in rat blood, versus potencies of 1222 nM and 2571 nM, respectively, for TNF inhibition. Likewise, BIRB796 showed an IC_{50} of 111 nM for IL-1β inhibition in human blood and 598 nM for IL-1β inhibition in rat blood, versus potencies of 579 nM and 974 nM, respectively, for TNF inhibition. SB203580 showed an IC_{50} of 158 nM for IL-1β inhibition in human blood and 677 nM for IL-1β inhibition in rat blood, versus potencies of 225 nM and 1691 nM, respectively, for TNF inhibition.

3.5. Specificity assays

Since most kinase inhibitors target the ATP site, specificity is a key issue. However, even though only a subset of the entire kinase family could be expected to adopt the DFG-out conformation to which allosteric or noncompetitive inhibitors such as KR-003048 bind, specificity was still of central concern during our lead optimization program. In addition, since binding specificity and affinity are not readily predicted based on available sequence and structural information, and current profiling methods are limited by the difficulty of

A

Inhibition of LPS-induced TNF secretion (nM) in human whole blood

SB203580			BIRB796			KR-003048		
mean	S.D.	n	mean	S.D.	n	mean	S.D.	n
225	266	6	579	316	10	1222	696	10

Inhibition of LPS-induced IL-1β secretion (nM) in human whole blood

SB203580			BIRB796			KR-003048		
mean	S.D.	n	mean	S.D.	n	mean	S.D.	n
158	69	6	111	57	6	408	237	6

Inhibition of LPS-induced TNF secretion (nM) in rat whole blood

SB203580			BIRB796			KR-003048		
mean	S.D.	n	mean	S.D.	n	mean	S.D.	n
1691	678	6	974	88	6	2571	579	6

Inhibition of LPS-induced IL-1β secretion (nM) in rat whole blood

SB203580			BIRB796			KR-003048		
mean	S.D.	n	mean	S.D.	n	mean	S.D.	n
677	429	9	598	480	8	2067	1338	8

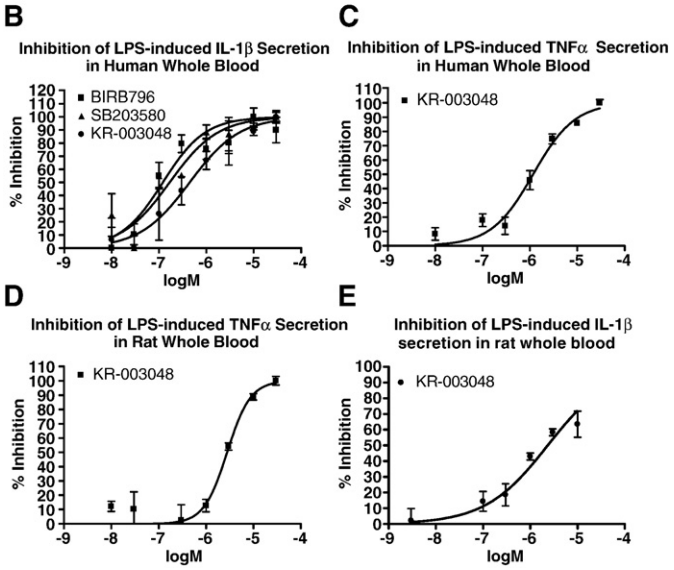

Fig. 6. A. Whole blood assay rat and human. Human or rodent whole blood diluted with media was exposed to LPS in the presence or absence of p38 MAP kinase inhibitors KR-003048, SB203580, and BIRB796. The release of cytokines IL-1b or TNF was measured, and IC_{50}s calculated. Tabulated data for all experiments performed with each compound are shown. B. Human whole blood assay. Human whole blood diluted with media was exposed to LPS in the presence or absence of p38 MAP kinase inhibitors KR-003048, SB203580, and BIRB796. The release of cytokines IL-1β was measured, and IC_{50}s calculated. Representative curves for all compounds for inhibition LPS-induced secretion of IL-1β from human whole blood are shown. C. Human whole blood assay. Human whole blood diluted with media was exposed to LPS in the presence or absence of p38 MAP kinase inhibitors KR-003048, SB203580, and BIRB796. The release of TNF was measured, and IC_{50}s calculated. A representative curve for KR-003048 is shown. D. Rat whole blood assay. Rat whole blood diluted with media was exposed to LPS in the presence or absence of p38 MAP kinase inhibitors KR-003048, SB203580, and BIRB796. The release of TNF was measured, and IC_{50}s calculated. A representative curve for KR-003048 is shown. E. Rat whole blood assay. Rat whole blood diluted with media was exposed to LPS in the presence or absence of p38 MAP kinase inhibitors KR-003048, SB203580, and BIRB796. The release of IL-1β was measured, and IC_{50}s calculated. A representative curve for KR-003048 is shown.

developing large numbers of kinase activity assays, we employed the outsourcing services offered by Cerep to understand the selectivity profile of our compound. The kinases listed in Table 1 were pre-incubated with KR-003048, SB203580, or BIRB796 at 10 μM, and then tested for their ability to phosphorylate their respective test substrates. Percentages inhibitions of maximal kinase activity under these conditions are enumerated in Table 1. As would be expected by its binding to the completely conserved ATP site, the competitive inhibitor SB203580 displays the least selectivity towards its intended target p38α. SB203580 is known to inhibit the p38α and β isoforms but not the γ and δ isoforms, and that is accurately reproduced in the work described here. All three p38 inhibitors tested inhibit the α isoform more strongly than the δ isoform. While all three compounds

Table 1
The kinases listed were pre-incubated with 10 μM KR-003048, SB203580, or BIRB796, then tested for their ability to phosphorylate their respective test substrates. Numbers in the table represent percentage inhibition of maximal kinase activity under these conditions. Experiments were conducted on a contract basis by Cerep.

	SB203580	BIRB796	KR-003048
Abl kinase (h)	36	19	−5
Akt1/ PKBalpha (h)	−30	−8	−2
AMPKalpha	12	−2	−7
BMX (Etk) kinase (h)	43	−1	1
Brk (h)	85	29	−10
CaMK2alpha (h)	7	8	−2
CaMK4 (h)	12	6	−2
CDC2/CDK1 (cycB) (h)	1	1	−5
CHK1 (h)	5	4	−4
CHK2 (h)	4	9	3
c-Met kinase (h)	23	4	−4
CSK (h)	47	29	−15
EGFR kinase (h)	96	42	−12
EphB4 kinase (h)	58	97	−5
ERK2 (P42mapk) (h)	4	4	0
FAK (h)	6	36	2
Fes kinase (h)	4	34	−17
FGFR1 kinase (h)	42	81	9
FLT-1 kinase (VEGFR1) (h)	74	97	10
FLT-3 kinase (h)	53	80	−25
IGF1R kinase (h)	1	1	1
IKKbeta (h)	2	−9	−11
IRK (InsR) (h)	5	15	−8
JAK3 (h)	28	9	−18
JNK 1 (h)	81	11	−14
JNK 2 (h)	93	99	87
KDR kinase (VEGFR2) (h)	88	100	87
Lck kinase (h)	17	28	−12
Lyn kinase (h)	90	91	−26
MAPKAPK2 (h)	7	1	3
MEK1 /MAP2K1 (h)	4	−6	1
p38alpha kinase (h)	98	99	99
p38delta kinase (h)	7	39	82
p70S6K (h)	38	−2	16
PDGFRbeta kinase (h)	83	82	7
PDK1 (h)	10	1	5
PKA (h)	18	−2	3
PKCalpha (h)	1	−1	−1
PKCgamma (h)	−7	−5	−4
ROCK2 (h)	14	5	4
RSK2 (h)	18	22	−4
Src kinase (h)	23	−12	−17
TRKA (h)	20	99	1
ZAP70 kinase (h)	12	12	−1

did not inhibit the MAP kinase ERK2, all did inhibit strongly the Jun N-terminal kinase 2 (JNK2) isoform of the third MAP kinase subfamily, the Jun N-terminal kinases, or JNKs. SB203580 also strongly inhibited the JNK1 isoform. SB203580 inhibited EGFR as well. Relative to KR-003048, both SB203580 and BIRB796 inhibited the receptor tyrosine kinases Eph receptor B4 (EphB4), vascular endothelial growth factor receptor (VEGFR), FMS-like tyrosine kinase 3 (FLT-3), platelet-derived growth factor receptor β (PDGFRβ) and non-receptor tyrosine kinase Lyn. BIRB796 displayed a singular inhibitory activity towards neurotrophic tyrosine kinase receptor type 1 (TRKA), while KR-003048 inhibited p38δ to significantly greater extent than did the other two p38 inhibitors tested.

3.6. Pharmacokinetics in rats

Since SB203580 was never advanced into clinical development, we chose to compare KR-003048 solely to the clinical compound BIRB796 when examining the former's preclinical *in vivo* properties. Snapshot pharmacokinetic parameters for both compounds were determined in male Lewis rats by comparing circulating exposures of both compounds at various times after oral and intravenous administration. Fig. 7 reports these results, which can be compared reasonably well

	KR-003048		BIRB796	
	30 mg/kg p.o.	5 mg/kg i.v.	20 mg/kg p.o.	10 mg/kg i.v.
$T_{1/2}$ (h)	4.7	5.1	3.2	4.9
AUC (ug*h/ml)	17.5	13.9	165	188
CL (ml/min/kg)	-	12	-	0.88
Vss (L/kg)	-	1.9	-	0.39
F(%)	49	-	44	-
C_{max} (ug/ml)	3.9	-	27	-
T_{max} (h)	0.5	-	0.5	-

Fig. 7. Pharmacokinetics. Snapshot pharmacokinetic parameters for both compounds were determined in male Lewis rats by comparing circulating exposures of both compounds at various times after oral and intravenous administration.

despite slightly different dosages per route. Both compounds display good oral bioavailability, at 49% and 44% for KR-003048 and BIRB796, respectively. Likewise, $T_{1/2}$'s of 4.7 and 3.2 h for both compounds approach an ideal of around 5 h, with a time of maximal concentration (T_{max}) of 0.5 h only slightly below the optimal 1–3 h range. Substantial differences appear when comparing exposures, though. KR-003048 yields a maximal concentration (C_{max}) of 3.9 μg/ml and an area under the curve (AUC) of 17.5 μg/h/ml, both well below the C_{max} of 27 μg/ml and AUC of 165 μg/h/ml for BIRB796. KR-003048 has a desirable clearance rate of 12 ml/min/kg, an order of magnitude greater than the 0.88 ml/min/kg shown by BIRB796. In addition, the volume of distribution of KR-003048, at 1.9 l/kg, is significantly larger than the 0.39 l/kg volume calculated for BIRB796.

3.7. In vivo LPS challenge

Demonstration of the ability of KR-003048 and BIRB796 to inhibit inflammatory cytokine production *in vivo* was accomplished by using Lewis rats challenged with LPS (1 mg/kg i.p.). As seen in Fig. 8A, KR-003048 given p.o. 30 min before LPS challenge inhibited the production of TNFα. 30 mg/kg KR-003048 resulted in inhibition of TNFα release relative to animals challenged with LPS in the absence of any p38 or other MAP kinase inhibitor, though the magnitude of this effect did not rise to the level of statistical significance. Likewise, Fig. 8A demonstrates that 20 mg/kg BIRB796 inhibited TNFα production from the majority of animals challenged with LPS after predosing with this compound. While BIRB796 appears to completely inhibit cytokine production in a larger fraction of animals than does KR-003048, the fact that these experiments were performed at separate times limits the ability to compare these results directly.

3.8. Inhibition of carrageenan-induced paw edema

Given the ability of KR-003048 to inhibit TNFα production *in vivo*, we chose to evaluate the effect of the compound in an acute inflammatory model. Edema in the rodent paw after local carrageenan injection is a well-understood model of acute inflammation, and thus KR-003048 was tested for its effects in this system. KR-003048 and BIRB796 at 3, 10, and 30 mg/kg were tested for their efficacy in this model, and the results are shown in Fig. 8B. Relative to the non-selective cyclooxygenase inhibitor indomethacin, both compounds demonstrated substantial ability to inhibit the carrageenan-induced edema when orally dosed prophylactically. KR-003048 first was tested on its own, and at 2, 4, and 6 h at 30 mg/kg dose was able to inhibit paw swelling by 14, 43, and 37%, respectively, while the non-selective COX inhibitor indomethacin at 5 mg/kg inhibited paw swelling by 0, 81, and 59%, respectively, in this run of the assay. BIRB796 was included in a second run of this assay, and the considerable variability of the carrageenan paw edema (CPE) format can observed in the run-to-run changes in the data obtained for both indomethacin and KR-003048. In this run, at 2, 4, and 6 h, 5 mg/kg indomethacin inhibited paw swelling by 49, 52, and 41%, while 30 mg/kg KR-003048 only managed inhibitions of 18, 4, and 15% at these same time points. BIRB796 was

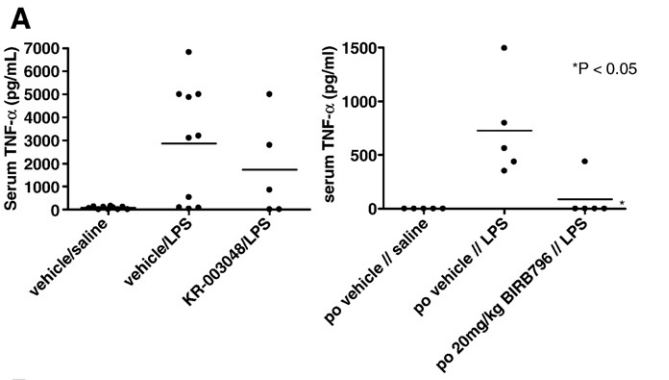

B

Treatment	0 Hour Percent Inhibition	2 Hour Percent Inhibition	3 Hour Percent Inhibition	4 Hour Percent Inhibition
Vehicle	0	0	0	0
5 mg/kg Indomethacin i.p.	0	0	81	59
30 mg/kg KR-003048 p.o.	0	14	43	37

Treatment	0 Hour Percent Inhibition	2 Hour Percent Inhibition	4 Hour Percent Inhibition	6 Hour Percent Inhibition
Vehicle	0	0	0	0
5 mg/kg Indomethacin i.p.	0	49	52	41
3 mg/kg BIRB796 p.o.	0	30	11	9
10 mg/kg BIRB796 p.o.	0	45	20	29
30 mg/kg BIRB796 p.o.	0	65	24	28
3 mg/kg KR-003048 p.o.	0	6	6	9
10 mg/kg KR-003048 p.o.	0	4	0	11
30 mg/kg KR-003048 p.o.	0	18	4	15

Fig. 8. A. *in vivo* LPS challenge in rats. KR-003048 and BIRB796 inhibit inflammatory cytokine production *in vivo* in Lewis rats challenged with LPS (1 mg/kg i.p.). B. Inhibition of carrageenan-induced paw edema. Edema in the rodent paw after local carrageenan injection can be blocked by inhibition of p38.

more efficacious at each time point at 30 mg/kg, displaying inhibitions of 65, 24, and 28%, respectively. Inhibitions at each time point at lower doses are also shown.

3.9. Inhibition of collagen-induced arthritis

Given the ability of KR-003048 to inhibit TNFα production and inflammatory paw swelling *in vivo*, it was of interest to evaluate the effect of the compound in a chronic inflammatory model. Collagen-induced arthritis was induced in DBA/1J mice by injection of bovine type II collagen at the base of the tail, followed 21 days later by a booster injection of collagen solubilized in acetic acid (i.p.). Animals with significant disease were treated for 14 days with KR-003048, BIRB796, or prednisolone. Every day, for 14 days, disease severity was judged on a scale of 0 to 4 per joint, and the group means for the summed scores of all animals were plotted over time. As seen in Fig. 9A both 30 mg/kg KR-003048 and 30 mg/kg BIRB796 significantly reduced disease severity ($P<0.05$) on the overall arthritic index endpoint. 10 mg/kg, despite a trend towards efficacy, did not achieve a statistically significant difference from untreated diseased animals ($P>0.05$).

KR-003048 displayed disease-modifying effects, as detailed in Fig. 9B. Contrary to the lack of statistical significance between disease untreated animals and animals treated with 10 mg/kg KR-003048, microscopic evaluation for signs of overall joint destruction revealed efficacy on this endpoint by this dose and the 30 mg/kg KR-003048 dose ($P<0.01$). 30 mg/kg BIRB796 also displayed efficacy on this microscopic endpoint ($P<0.01$). 30 mg/kg KR-003048 and BIRB796 reduced bone erosion ($P<0.05$), synovitis ($P<0.05$), and cartilage damage and thinning ($P<0.05$). All test article groups showed significant efficacy ($P<0.01$) against edema and inflammatory cell infiltrate count. Conversely, no test article showed efficacy ($P>0.05$) against periosteal bone formation. Interestingly, neither dose of KR-

003048 showed efficacy against pannus formation, whereas 30 mg/kg BIRB796 was able to modify this endpoint ($P<0.01$). No significant signs of tissue necrosis or fibroplasias were seen in any experimental groups.

4. Discussion

Pyridinylimidazole structures that inhibited IL-1β and TNFα production were labeled cytokine-suppressing anti-inflammatory drugs (CSAIDs) when first discovered, but later studies showed that the target molecule of these compounds was p38 MAP kinase (Han et al., 1993, 1994; Lee et al., 1994). p38 MAP kinase regulates the synthesis of cytokine, cyclooxygenase-2 (COX-2), and inducible nitric oxide synthase (iNOS) mediators of inflammatory processes (Badger, et al., 1996, 1998; McGinty et al., 2000; Faour, et al., 2001), and thus inhibitors of p38 MAP kinase may act as anti-inflammatory agents. Our results indicate the potential of KR-003048 as an anti-inflammatory agent.

KR-003048 potently inhibited TNFα production from an LPS-activated THP-1 immortalized monocyte cell line (Fig. 3A), and selectively inhibited the enzymatic activity of the α isoform of p38 (Fig. 4B and Table 1). KR-003048's p38 inhibition was approximately equipotent with the literature standard SB203580 and the clinical compound BIRB796. BIRB796's apparent cellular potency was roughly a half-log better than that of KR-003048 or SB203580. These differences could simply reflect an insufficient sampling of the true experimental situation; however, it is possible that these numerical differences reflect a true physical reality, in which case differential intracellular exposure to the compounds, due to differences in membrane permeability, intracellular metabolism of the compounds, transport of the compounds out of the cell, or binding to nontarget proteins, could account for the different potencies.

Boehringer's BIRB796 functions as a noncompetitive enzyme inhibitor by stabilizing a conformation of the protein (DFG-out) that is incompatible with ATP binding (Pargellis et al., 2002); others have shown that SB203580 binds to the catalytically active, DFG-in conformation of p38 (Tong et al., 1997). The conformational change resulting from BIRB796's noncompetitive mechanism of inhibition can be read out in its equipotent inhibition of phosphorylation of p38 by its upstream activating kinases (Fig. 5A) and inhibition of p38 catalytic activity measured both in cells (Fig. 3A) and biochemically (Fig. 4A). Conversely, SB203580 binds to the same conformational state of p38 as does ATP and competitively inhibits p38's catalytic activity in cells (Fig. 3A) and biochemically (Fig. 4A) with several logs lesser potency

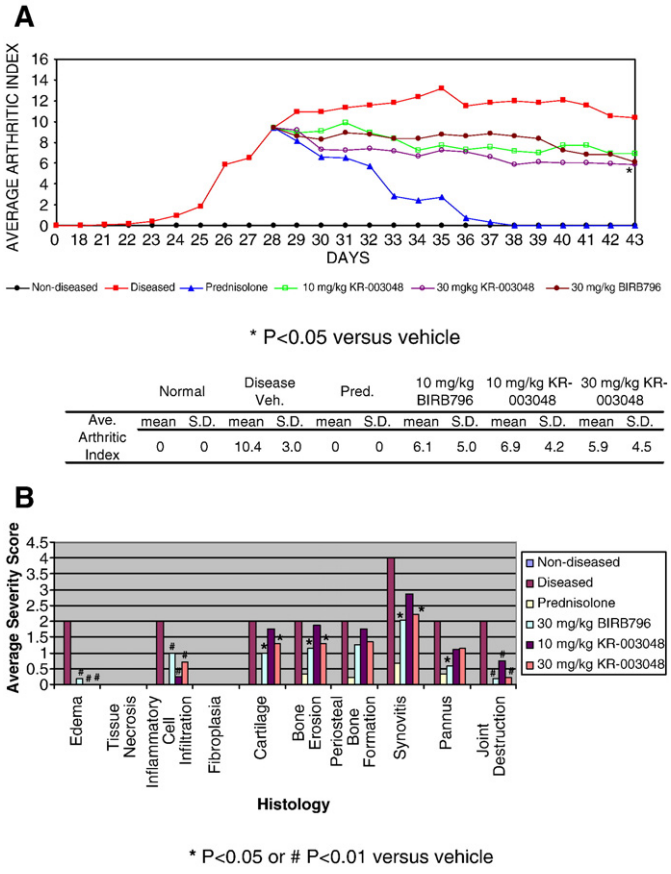

	Normal		Disease Veh.		Pred.		10 mg/kg BIRB796		10 mg/kg KR-003048		30 mg/kg KR-003048	
Ave. Arthritic Index	mean	S.D.	mean	S.D.	mean	S.D.	mean	S.D.	mean	S.D.	mean	S.D.
	0	0	10.4	3.0	0	0	6.1	5.0	6.9	4.2	5.9	4.5

Fig. 9. A. Inhibition of collagen-induced arthritis in mice. Collagen-induced arthritis induced in DBA/1J mice by injection of bovine type II collagen at the base of the tail followed 21 days later by a booster injection of collagen is inhibited by KR-003048 and BIRB796. Disease scores on the final day were compared by one-way ANOVA followed by Dunnett's multiple comparison test (vehicle-treated, diseased animals as control group). B. Disease-modifying effects of p38 inhibition during collagen-induced arthritis. KR-003048 and BIRB796 displayed disease-modifying effects when their effects on tissue were examined histopathologically. C. Normal, An 5, Ankle, 25×. Ankle from mouse in group 1 shows normal synovium (S) and normal tarsal joints (arrow). D. Vehicle, An 7, Ankle, 25×. Ankle from mouse treated with vehicle (with approximate mean score for the group) has moderate synovitis (S), mild pannus and bone destruction (small arrow) and marked overall cartilage loss that was always more severe in small tarsal joints (arrow). E. Prednisolone, An 6, Ankle, 25×. Ankle from mouse treated with Pred (with approximate mean score for the group) has minimal synovitis (S), no pannus and bone destruction and no cartilage loss. F. BIRB796 30 mg/kg, An 14, Ankle, 25×. Ankle from mouse treated with BIRB796—30 mg/kg (with approximate mean score for the group) has moderate synovitis (S), mild pannus and bone destruction (small arrow) and severe overall cartilage loss that was always more severe in small tarsal joints (arrow). G. KR-003048 10 mg/kg, An 9, Ankle, 25×. Ankle from mouse treated with 3048-10 mg/kg (with approximate mean score for the group) has marked synovitis (S), mild pannus and bone destruction (small arrow) and severe overall cartilage loss that was always more severe in small tarsal joints (arrow). H. KR-003048 30 mg/kg, An 13, Paw, 25×. Paw from mouse treated with 3048—30 mg/kg (with approximate mean score for the group) has marked synovitis (S), marked pannus and bone destruction (small arrow) and marked overall cartilage loss (arrow).

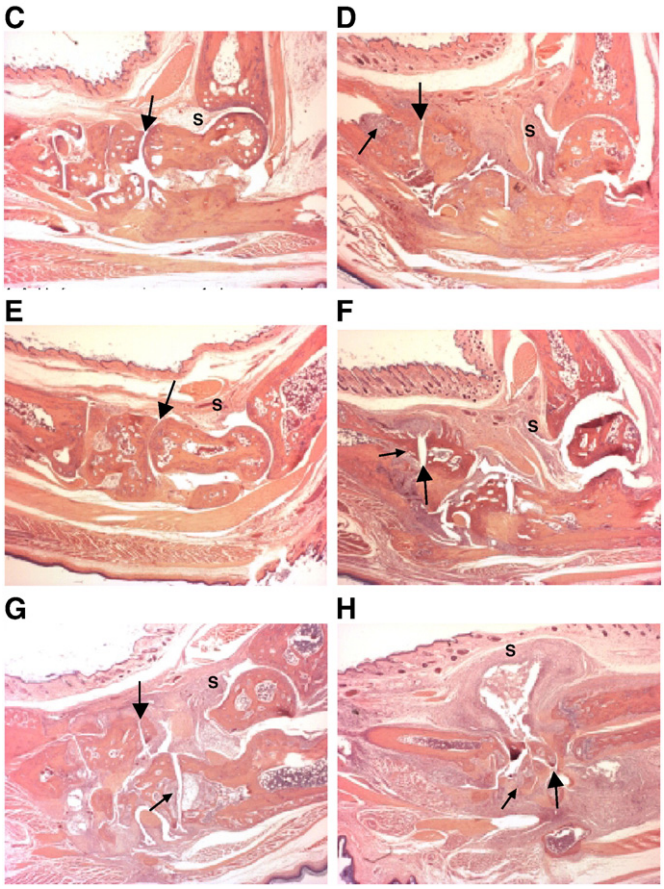

Fig. 9 (*continued*).

than it inhibits the conformationally-dependent phosphorylation of p38 by upstream kinases (Fig. 5A). Significantly, the potency of KR-003048 for inhibiting the phosphorylation of p38 (Fig. 5A) is very similar to its IC_{50} for inhibition of p38's catalytic activity measured both in cells (Fig. 3A) and biochemically (Fig. 4A), supporting a noncompetitive mechanism of inhibition of p38 via stabilization of the DFG-out, catalytically inactive conformation of the kinase.

KR-003048 displayed insignificant inhibition of almost all off-target kinases. Significant inhibition of the δ isoform of p38 was seen, as well as reactivity against both JNK2 and VEGFR2, which though substantial were not similar to the almost 100% inhibition of p38α at this concentration (Table 1). Both SB203580 and BIRB796 displayed an overall greater propensity towards off-target kinase inhibition (Table 1). Since these are not comparisons of potencies of inhibition for each compound on each enzyme, care should be exercised when making conclusions about the relative specificities of these three compounds. Nevertheless, with this caveat in mind and the knowledge that apparent potencies on p38 were roughly similar, it is tempting to speculate that KR-003048 is at least as specific as BIRB796 and SB203580 with respect to this set of kinases.

Cytokine inhibition in rat and human whole blood was utilized as a surrogate for physiologic conditions (Fig. 6). KR-003048 and BIRB796 were roughly equipotent in their inhibition of TNF release from both rat and human blood: KR-003048 displayed an IC_{50} of 1222 nM for TNF inhibition from human blood and 2571 nM from rat blood, while BIRB796 showed an IC_{50} of 579 nM for TNF inhibition from human blood and 974 nM from rat blood. Of note, SB203580 displayed an IC_{50} of 225 nM for inhibition of TNF from human blood and 1691 nM in rat blood, almost one log less in potency. This species difference in sensitivity only to SB203580 could be related to species differences in the amino acid sequences of p38α and the differing binding modes of the allosteric kinase inhibitors KR-003048 and BIRB796 versus that of the direct ATP competitor SB203580. The human sequence (Han et al., 1994) diverges at 5 positions from the rat p38α protein sequence (Nemeth et al., 1998). Crucially, one of the differences is a leucine-to-histidine change at residue 48 in the rat protein, thereby introducing a basic amino acid with a bulkier group close to residue 51. Cocrystals of p38 and SB203580 have shown the latter to be a point of contact with the p-fluorophenyl moiety of pyridinylimidazoles (Wilson et al., 1997).

KR-003048, SB203580, and BIRB796 all were more potent in their inhibition of IL-1β secretion by LPS-stimulated blood than in the corresponding inhibition of TNF secretion, for reasons that are not clear at this time.

Bacterial lipopolysaccharide is a well-known activator of p38 MAP kinase. In this study, separate experiments with 30 mg/kg KR-003048 and 20 mg/kg BIRB796 inhibited TNFα release in LPS-treated rats. Interestingly, despite roughly similar potencies on the molecular target and a higher administered dose, KR-003048 was less efficacious in its cytokine inhibition than was BIRB796 (Fig. 8A), and did not rise to the level of a statistically significant effect despite an encouraging trend in this direction. There are several possible explanations for this discrepancy. First, KR-003048 may be poorly absorbed and/or rapidly metabolized in rodents. Pharmacokinetic data generated in other experiments suggest an equivalent oral bioavailability, T_{max}, and oral half-lives (Fig. 7), arguing against differences in absorption. However, these same data do reveal a substantial greater exposure to compound when 20 mg/kg BIRB796 is administered than when 30 mg/kg KR-003048 is administered. KR-003048 is cleared more rapidly and has a greater volume of distribution that BIRB796, raising the possibility of greater binding of BIRB796 to rat plasma proteins. Both compounds exhibit very high levels of plasma protein binding *in vitro* (data not shown), making accurate comparison of the two compounds on this endpoint difficult.

TNFα plays a central role in carrageenan-induced paw edema as well (Sekut et al., 1994). In this study, prophylactic treatment with either of the p38 inhibitors KR-003048 or BIRB796 resulted in inhibition of the paw edema induced by carrageenan (Fig. 8B). The dose-proportionality of both compounds in the studies reported was weak, but 30 mg/kg doses were clearly more efficacious than 3 mg/kg doses in all instances.

Collagen-induced arthritis in DBA/1J mice is an arthritis model in which synovial infiltration and joint destruction similar to those of human rheumatoid arthritis are seen (Stuart et al., 1982). We tested the therapeutic effects of KR-003048 and BIRB796 in the animals with severe symptoms (Fig. 9A), because efficacy in established arthritis is more relevant to eventual clinical application than is prophylactic treatment or inhibition of progression from mild to moderate disease. Over a 14-day dosing period, 10 and 30 mg/kg KR-003048 and 30 mg/kg BIRB796 prevented progression of the signs of underlying arthritis. The contribution of proinflammatory cytokines to collagen-induced arthritis has been reported in previous studies using transgenic mice deficient in IL-6 (Alonzi et al., 1998; Sasai et al., 1999; Campbell et al., 2001), or cytokine blockades that include anti-IL-1 receptor (IL-1R) or anti-TNFα antibodies (Williams et al., 2000). Given that both KR-003048 and BIRB796 displayed suppression of both cytokines *in vitro*, simultaneous suppression of these cytokines may have led to this complete block of disease progression.

Histological analysis (Fig. 9B) showed that both KR-003048 and BIRB796 ameliorated bone erosion, synovitis, cartilage thinning and damage, edema, and inflammatory cell infiltration, whereas only BIRB796 revealed an observable effect on pannus formation upon microscopic observation. Fig. 9C–H contains annotated photomicrographs of the stained joints of a typical animal from each treatment group in the study. As in the human state, such symptoms in bone and cartilage tissues of untreated diseased animals emphasize the ongoing process of joint destruction in the arthritis model; conversely, the fact that the p38 inhibitors KR-003048 and BIRB796 both can halt the progression of microscopic signs of disease strongly argues for their potential to be disease-modifying agents clinically as well.

In summary, we have shown that KR-003048 is a potent inhibitor of the p38 MAP kinase signaling pathway *in vitro* and *in vivo*. KR-00348 was demonstrated to be a potent inhibitor of inflammatory cytokine production *ex vivo* in rat and human whole blood, and showed good oral bioavailability. Additionally, efficacy in mouse and rat models of acute and chronic inflammation was obtained. Evidence for disease-modifying activity in this model was indicated by histological evaluation of joints. Because of a similarly favorable pharmacological profile, an analogue of KR-003048 was advanced into clinical development and has completed Phase II clinical trials in rheumatoid arthritis and pemphigus vulgaris in an oral formulation, and was advanced into preclinical development in a topical formulation for mild to moderate psoriasis.

Acknowledgements

We thank Washington Biotechnology (Guilford, Maryland) for providing contract research services of collagen-induced arthritis and carrageenan-induced paw edema animal models, Bolder BIOpath (Boulder Colorado) for providing the contract research services of histopathology, Perry Scientific (San Diego, California) for providing the contract research services of pharmacokinetics and LPS challenge studies, and Calvert Laboratories (Olyphant, Pennsylvania) for providing contract research services of carrageenan-induced paw edema. All animal protocols were approved by the ethics committee (s) of the respective institution/vendor.

References

Alonzi, T., Fattori, E., Cappelletti, M., Ciliberto, G., Poli, V., 1998. Impaired Stat3 activation following localized inflammatory stimulus in IL-6-deficient mice. Cytokine 10, 13–18.

Badger, A.M., Bradbeer, J.N., Votta, B., Lee, J.C., Adams, J.L., Griswold, D.E., 1996. Pharmacological profile of SB 203580, a selective inhibitor of cytokine suppressive

binding protein/p38 kinase, in animal models of arthritis, bone resorption, endotoxin shock and immune function. J. Pharmacol. Exp. Ther. 279, 1453–1461.
Badger, A.M., Cook, M.N., Lark, M.W., Newman-Tarr, T.M., Swift, B.A., Nelson, A.H., Barone, F.C., Kumar, S., 1998. SB 203580 inhibits p38 mitogen-activated protein kinase, nitric oxide production, and inducible nitric oxide synthase in bovine cartilage-derived chondrocytes. J. Immunol. 161, 467–473.
Bingham III, C.O., 2002. The pathogenesis of rheumatoid arthritis: pivotal cytokines involved in bone degradation and inflammation. J. Rheumatol. Suppl. 65, 3–9.
Campbell, I.K., O'Donnell, K., Lawlor, K.E., Wicks, I.P., 2001. Severe inflammatory arthritis and lymphadenopathy in the absence of TNF. J. Clin. Invest. 107, 1519–1527.
de Winter, R.J., Tijssen, J.G.P., Windhaussen, F., Slagboom, T., Krasznai, K., Michels, H.R., Dunselman, P.H.J.M., vant Hof, A.N.G., Bosschaert, M., Suttorp, M.J., Merica, E., Godfrey, C.J., Ogenstad, S., Williams, L., Martin-Munley, S., Kauffman, R., Mohanlal, R., 2005. A major determinant of C-reactive protein production in patients with acute coronary syndrome undergoing PCI: the p38 mitogen activated protein kinase pathway. American Heart Association Scientific Sessions, Dallas, Texas.
Diller, D.J., Lin, T.H., Metzger, A., 2005. The discovery of novel chemotypes of p38 kinase inhibitors. Curr. Top. Med. Chem. 5, 953–965.
Dominguez, C., Tamayo, N., Zhang, D., 2005. p38 inhibitors: beyond pryidinylimidazoles. Expert Opin. Ther. Pat. 15, 801–816.
Faour, W.H., He, Y., He, Q.W., de, L.M., Quintero, M., Mancini, A., Di Battista, J.A., 2001. Prostaglandin E(2) regulates the level and stability of cyclooxygenase-2 mRNA through activation of p38 mitogen-activated protein kinase in interleukin-1 beta-treated human synovial fibroblasts. J. Biol. Chem. 276, 31720–31731.
Garrido Montalban, A., Boman, E., Chang, C.-D., Conde Ceide, S., Dahl, R., Dalesandro, D., Delaet, N.G.J., Erb, E., Ernst, J.T., Gibbs, A., Kahl, J., Kessler, L., Lundström, J., Miller, S., Nakanishi, H., Roberts, E., Saiah, E., Sullivan, R., Wang, Z., Larson, C.J., 2008. The design and synthesis of novel alpha-ketoamide-based p38 MAP kinase inhibitors. Bioorg. Med. Chem. Lett. 18, 1772–1777.
Han, J., Lee, J.D., Tobias, P.S., Ulevitch, R.J., 1993. Endotoxin induces rapid protein tyrosine phosphorylation in 70Z/3 cells expressing CD14. J. Biol. Chem. 268, 25009–25014.
Han, J., Lee, J.D., Bibbs, L., Ulevitch, R.J., 1994. A MAP kinase targeted by endotoxin and hyperosmolarity in mammalian cells. Science 265, 808–811.
Hannigan, M.O., Zhan, L., Ai, Y., Kotlyarov, A., Gaestel, M., Huang, C.K., 2001. Abnormal migration phenotype of mitogen-activated protein kinase-activated protein kinase 2−/− neutrophils in Zigmond chambers containing formyl-methionyl-leucyl-phenylalanine gradients. J. Immunol. 167, 3953–3961.
Herlaar, E., Brown, Z., 1999. p38 MAPK signalling cascades in inflammatory disease. Mol. Med. Today 5, 439–447.
Hynes Jr., J., Leftheri, K., 2005. Small molecule p38 inhibitors: novel structural features and advances from 2002–2005. Curr. Top. Med. Chem. 5, 967–985.
Kontoyiannis, D., Boulougouris, G., Manoloukos, M., Armaka, M., Apostolaki, M., Pizarro, T., Kotlyarov, A., Forster, I., Flavell, R., Gaestel, M., Tsichlis, P., Cominelli, F., Kollias, G., 2002. Genetic dissection of the cellular pathways and signaling mechanisms in modeled tumor necrosis factor-induced Crohn's-like inflammatory bowel disease. J. Exp. Med. 196, 1563–1574.
Kotlyarov, A., Yannoni, Y., Fritz, S., Laass, K., Telliez, J.B., Pitman, D., Lin, L.L., Gaestel, M., 2002. Distinct cellular functions of MK2. Mol. Cell. Biol. 22, 4827–4835.
Kyriakis, J.M., Avruch, J., 1996. Sounding the alarm: protein kinase cascades activated by stress and inflammation. J. Biol. Chem. 271, 24313–24316.
Kyriakis, J.M., Banerjee, P., Nikolakaki, E., Dai, T., Rubie, E.A., Ahmad, M.F., Avruch, J., Woodgett, J.R., 1994. The stress-activated protein kinase subfamily of c-Jun kinases. Nature 369, 156–160.
Lee, J.C., Laydon, J.T., McDonnell, P.C., Gallagher, T.F., Kumar, S., Green, D., McNulty, D., Blumenthal, M.J., Heys, J.R., Landvatter, S.W., 1994. A protein kinase involved in the regulation of inflammatory cytokine biosynthesis. Nature 372, 739–746.
McGinty, A., Foschi, M., Chang, Y.W., Han, J., Dunn, M.J., Sorokin, A., 2000. Induction of prostaglandin endoperoxide synthase 2 by mitogen-activated protein kinase cascades. Biochem. J. 352 (Pt 2), 419–424.
Michelotti, E.L., Moffett, K.K., Nguyen, D., Kelly, M.J., Shetty, R., Chai, X., Northrop, K., Namboodiri, V., Campbell, B., Flynn, G.A., Fujimoto, T., Hollinger, F.P., Bukhtiyarova, M., Springman, E.B., Karpusas, M., 2005. Two classes of p38alpha MAP kinase inhibitors having a common diphenylether core but exhibiting divergent binding modes. Bioorg. Med. Chem. Lett. 15, 5274–5279.
Natarajan, S.R., Doherty, J.B., 2005. P38 MAP kinase inhibitors: evolution of imidazole-based and pyrido-pyrimidin-2-one lead classes. Curr. Top. Med. Chem. 5, 987–1003.
Nemeth, E., Bole-Feysot, C., Tashima, L.S., 1998. Suppression subtractive hybridization (SSH) identifies prolactin stimulation of p38 MAP kinase gene expression in Nb2 T lymphoma cells: molecular cloning of rat p38 MAP kinase. J. Mol. Endocrinol. 20, 151–156.
Ono, K., Han, J., 2000. The p38 signal transduction pathway: activation and function. Cell. Signal. 12, 1–13.
Pargellis, C., Regan, J., 2003. Inhibitors of p38 mitogen-activated protein kinase for the treatment of rheumatoid arthritis. Curr. Opin. Investig. Drugs 4, 566–571.
Pargellis, C., Tong, L., Churchill, L., Cirillo, P., Gilmore, T., Graham, A., Grob, P., Hickey, E., Moss, N., Pav, S., Regan, J., 2002. Inhibition of p38 MAP kinase by utilizing a novel allosteric binding site. Nat. Struct. Biol. 9, 268–272.
Redlich, K., Schett, G., Steiner, G., Hayer, S., Wagner, E., Smolen, J., 2003. Rheumatoid arthritis therapy after tumor necrosis factor and interleukin-1 blockade. Arthritis Rheum. 48, 3308–3319.
Regan, J., Breitfelder, S., Cirillo, P., Gilmore, T., Graham, A., Hickey, E., Klaus, B., Madwed, J., Moriak, M., Moss, N., Pargellis, C., Pav, S., Proto, A., Swinamer, A., Tong, L., Torcellini, C., 2002. Pyrazole urea-based inhibitors of p38 MAP kinase: from lead compound to clinical candidate. J. Med. Chem. 45, 2994–3008.
Regan, J., Capolino, A., Cirillo, P., Gilmore, T., Graham, A., Hickey, E., Kroe, R., Madwed, J., Moriak, M., Nelson, R., Pargellis, C., Swinamer, A., Torcellini, C., Tsang, M., Moss, N., 2003. Structure–activity relationships of the p38r MAP kinase inhibitor 1-(5-tert-Butyl-2-p-tolyl-2H-pyrazol-3-yl)-3-[4-(2-morpholin-4-yl-ethoxy)naphthalen-1-yl]urea (BIRB 796). J. Med. Chem. 46, 4676–4686.
Saklatvala, J., 2004. The p38 MAP kinase pathway as a therapeutic target in inflammatory disease. Curr. Opin. Pharmacol. 4, 372–377.
Sasai, M., Saeki, Y., Ohshima, S., Nishioka, K., Mima, T., Tanaka, T., Katada, Y., Yoshizaki, K., Suemura, M., Kishimoto, T., 1999. Delayed onset and reduced severity of collagen-induced arthritis in interleukin-6-deficient mice. Arthritis Rheum. 42, 1635–1643.
Schreiber, S., Feagan, B., D'Haens, G., Colombel, J.F., Geboes, K., Yurcov, M., et al., 2006. Oral p38 mitogen-activated protein kinase inhibition with BIRB 796 for active Crohn's disease: a randomized, double-blind, placebo-controlled trial. Clin. Gastroenterol. Hepatol. 4, 325–334.
Sekut, L., Menius Jr., J.A., Brackeen, M.F., Connolly, K.M., 1994. Evaluation of the significance of elevated levels of systemic and localized tumor necrosis factor in different animal models of inflammation. J. Lab. Clin. Med. 124, 813–820.
Shi, Y., Gaestel, M., 2002. In the cellular garden of forking paths: how p38 MAPKs signal for downstream assistance. Biol. Chem. 383, 1519–1536.
Stuart, J.M., Cremer, M.A., Townes, A.S., Kang, A.H., 1982. Type II collagen-induced arthritis in rats. Passive transfer with serum and evidence that IgG anticollagen antibodies can cause arthritis. J. Exp. Med. 155, 1–16.
Tong, L., Pav, S., White, D., Rogers, S., Crane, K., Cywin, C., Brown, M., Pargellis, C., 1997. A highly specific inhibitor of human p38 MAP kinase binds in the ATP pocket. Nat. Struct. Biol. 4, 311–316.
Waetzig, G., Seegert, D., Rosenstiel, P., Nikolaus, S., Schreiber, S., 2002. p38 mitogen-activated protein kinase is activated and linked to TNF-α signaling in inflammatory bowel disease. J. Immunol. 168, 5342–5351.
Wang, X., Xu, L., Wang, H., Young, P.R., Gaestel, M., Feuerstein, G.Z., 2002. Mitogen-activated protein kinase-activated protein (MAPKAP) kinase 2 deficiency protects brain from ischemic injury in mice. J. Biol. Chem. 277, 43968–43972.
Weisman, M., Furst, D., Schiff, M., Kauffman, R., Merica, E., Martin-Munley, S., 2002. A double-blind, placebo-controlled trial of VX-745, an oral p38 mitogen activated protein kinase (MAPK) inhibitor, in patients with rheumatoid arthritis. Official meeting of the European League Against Rheumatism, Annual European Congress of Rheumatology, Stockholm, Sweden.
Williams, R.O., Feldmann, M., Maini, R.N., 2000. Cartilage destruction and bone erosion in arthritis: the role of tumour necrosis factor alpha. Ann. Rheum. Dis. 59 (Suppl 1), i75–i80.
Wilson, K.P., McCaffrey, P.G., Hsiao, K., Pazhanisamy, S., Galullo, V., Bemis, G.W., Fitzgibbon, M.J., Caron, P.R., Murcko, M.A., Su, M.S., 1997. The structural basis for the specificity of pyridinylimidazole inhibitors of p38 MAP kinase. Chem. Biol. 4, 423–431.